Modified Distance-based Subset Selection for Evolutionary Multi-objective Optimization Algorithms

Weiyu Chen, Hisao Ishibuchi, Ke Shang
Shenzhen Key Laboratory of Computational Intelligence,
University Key Laboratory of Evolving Intelligent Systems of Guangdong Province,
Department of Computer Science and Engineering, Southern University of Science and Technology (SUSTech),
Shenzhen, China
11711904@mail.sustech.edu.cn, hisao@sustech.edu.cn, kshang@foxmail.com

***Abstract*—Evolutionary algorithms have been widely used to solve multi-objective optimization problems. Usually, the final population of an evolutionary algorithm is used as the output of multi-objective optimization. However, a current new trend is to select a pre-specified number of solutions from an unbounded external archive (UEA) as the final output of multi-objective optimization. Some subset selection methods have been proposed in the literature such as hypervolume-based and IGD-based selection. Recently, a distance-based subset selection (DSS) method was proposed for efficient subset selection from a large external archive. Whereas DSS efficiently finds a set of uniformly distributed solutions, it has some difficulties in the handling of solutions in the UEA as we demonstrate in this paper. To improve the performance of the DSS method, we propose a modified DSS method based on the IGD^+ distance instead of the Euclidean distance. Experimental results on various benchmark problems show that the modified DSS method performs better than or equal to the original DSS method on most test problems.**

***Index Terms*—Evolutionary multi-objective optimization, distance-based solution subset selection, unbounded external archive**

I. Introduction

In the last three decades, many evolutionary multi-objective optimization (EMO) algorithms have been proposed. They can be roughly divided into three categories: (i) Pareto dominance-based algorithms (e.g., NSGA-II [1], NSGA-III [2]), (ii) decomposition-based algorithms (e.g., MOEA/D [3], RVEA [4]) and (iii) indicator-based algorithms (e.g., IBEA [5], BiGE [6]). In most papers, the final population of an algorithm is chosen as the Pareto front (PF) approximation of a multi-objective optimization problem. This is intuitive since EMO algorithms are usually designed to improve the convergence and the diversity of the current population over generations.

This work was supported by National Natural Science Foundation of China (Grant No. 61876075), the Program for Guangdong Introducing Innovative and Entrepreneurial Teams (Grant No. 2017ZT07X386), Shenzhen Peacock Plan (Grant No. KQTD2016112514355531), the Science and Technology Innovation Committee Foundation of Shenzhen (Grant No. ZDSYS201703031748284), and the Program for University Key Laboratory of Guangdong Province (Grant No. 2017KSYS008).

Corresponding Author: Hisao Ishibuchi (hisao@sustech.edu.cn)

However, as pointed out in [7], [8], a better PF approximation may exist within an unbounded external archive (UEA) which stores non-dominated solutions among the evaluated solutions. Therefore, selecting a pre-specified number of well-distributed solutions from a large number of non-dominated solutions in the UEA may lead to a better PF approximation.

Many subset selection methods have been proposed to select a pre-specified number of solutions from a large number of non-dominated solutions. Among them, hypervolume-based methods are widely used [9]–[11]. They can be further classified into three categories: (i) exact optimization methods, (ii) greedy inclusion/removal methods, and (iii) genetic algorithm-based methods. These methods can find good solution subsets. However, they also have high computational complexity since the calculation of the hypervolume is a #P-hard problem [12]. When we have a large solution set of a many-objective problem (e.g., all the examined solutions by an EMO algorithm on a 20-objective problem), the computation time of these methods can be impractically large.

Recently, Tanabe et al. [7] proposed a distance-based subset selection (DSS) method by modifying a similar method in [13]. In each iteration, the DSS method finds an unselected solution which has the largest Euclidean distance from the selected solution set. Then the solution is added to the selected solution set. This procedure is iterated until the required number of solutions are selected. The DSS method was theoretically analyzed by Singh et al. [14]. They showed that the selected solution set by the DSS method from an infinitely large number of points on the true PF is conditionally equivalent to the optimal solution subset for hypervolume maximization.

The main contributions of this paper are as follows:

1) Through computational experiments, we demonstrate that selected solutions from the UEA by the DSS method can be inferior to the final population. Then we clearly show the reason for the negative effect of solution selection.
2) We propose a modified distance-based subset selection method to remedy the negative effect of the DSS

method. The proposed method is based on the IGD^+ distance instead of the Euclidean distance to select a better solution subset.

The rest of this paper is organized as follows. In section II, we demonstrate the negative effect of solution selection by the DSS method through computational experiments and explain its reason. In section III we propose a modified distance-based subset selection method and demonstrate its usefulness through computational experiments. Finally, we conclude this paper in section IV.

II. Distance-based Subset Selection and its Drawbacks

A. Distance-based Subset Selection

Since good solutions can be discarded during multi-objective evolution, selected solutions from the UEA can be better than the final population. The DSS method [7], [14] is proposed to efficiently select a pre-specified number of solutions from a large number of non-dominated solutions in the UEA. In each iteration, the solution that has the largest Euclidian distance from the selected solution set is found until the required number of solutions are selected. Comparing with hypervolume-based selection, the DSS method has lower computational complexity. We can quickly complete solution selection even when a large number of non-dominated solutions are included in the UEA. The details of the DSS method are shown in Algorithm 1, which is the same as in [14].

Algorithm 1 Distance-Based Subset Selection (DSS)

Input: A (A set of non-dominated solutions in UEA), k (Solution subset size)
Output: P (A set of selected solutions)

if $|A| < k$ **then**
  $P = A$
else
  Normalize all solutions in A to $[0, 1]$
  Sort A based on the crowding distance
  Initialize P as the first solution in the sorted archive A
  while $|A| < k$ **do**
    for each a_i in $A \setminus P$ **do**
      D_i= minimum Euclidean distance from a_i to any point in P
    end for
    Choose solution from $A \setminus P$ associated with the largest Euclidean distance and add it to P
  end while
end if

B. Difficulties in the Distance-based Subset Selection

1) Experimental Settings

To examine the performance of the DSS method for different EMO algorithms and different test problems, we choose 11 representative test problems with various PF shapes: four test problems with a regular PF, four test problems with an inverted triangle PF, two test problems with a discontinuous PF, and one test problem with a degenerated PF. The details of the PF shape of each test problem is shown in Table I.

TABLE I
Pareto Front Shapes of Benchmark Problems

Problem	Pareto Front Geometry
DTLZ1 [15]	Linear triangular
DTLZ2 [15]	Concave
DTLZ3 [15]	Concave
DTLZ4 [15]	Concave
DTLZ1-1 [16]	Inverted triangular
DTLZ2-1 [16]	Inverted quadratic (convex)
mDTLZ1 [17]	Inverted triangular
mDTLZ2 [17]	Inverted quadratic (convex)
DTLZ7 [15]	Discontinuous
WFG2 [18]	Discontinuous
DTLZ5IM [19]	Degenerate

mDTLZ1 and mDTLZ2 [17] are recently proposed new test problems. They do not have the following special characteristics of almost all traditional test problems: (1) the Pareto front shape is regular, and (2) all objective functions have the same distance function. They have large hardly dominated regions (with dominance resistant solutions) in the objective space.

To examine the effect of the DSS method, we choose three EMO algorithms: NSGA-III [2], BiGE [15] and MOEA/D with the Tchebycheff function [3]. All non-dominated solutions among the examined solutions in each run of each algorithm are stored in the UEA. Then the DSS method is applied to the UEA.

Following the suggestion of Deb et al. [15], the number of variables is set to $(M + k - 1)$, where M is the number of objectives and k is the number of distance variables. k is set to 5 for DTLZ1, DTLZ1^{-1} and mDTLZ1 while it is set to 10 for the other test problems. For each $M \in \{3, 5, 8\}$, we set the population size to 91, 210 and 156, respectively, for MOEA/D and BiGE, while 92, 212, 156 for NSGA-III. These settings are exactly the same as in NSGA-II paper [2]. The number of function evaluations is used as the termination condition of each algorithm: 30,000 for three-objective problems, 60,000 for five-objective problems, and 100,000 for eight-objective problems.

Polynomial mutation and simulated binary crossover (SBX) [20] are used in each algorithm. We set the SBX probability to 1 and the polynomial mutation probability to $1/n$, where n is the number of variables. The distribution index is specified as 20 in both polynomial mutation and SBX.

The hypervolume (HV) indicator [21] is chosen to compare the selected solutions and the final population of each algorithm. The reference point for hypervolume calculation is specified as (1.1, 1.1, ...,1.1).

Each algorithm is executed 31 times for each test problem. Experimental results are analyzed by the Wilcoxon rank sum test with a significance level of 0.05 to check whether one method is statistically significantly better than another method. The test results are shown by "+", "-" and "=" where "+", "-" and "=" indicate that one method is "significantly better than",

"significantly worse than" and "not significantly different from" another method, respectively.

2) Experimental Results

Table II shows the average HV value of the final population and the selected solutions by the DSS method over 31 runs of each EMO algorithm. The number of selected solutions is the same as the population size. The bolded value in Table II indicates that one method (the final population or the selected solutions) is significantly better than the other by the Wilcoxon rank sum test. The bottom line shows the summary.

From Table II, the following observations can be obtained:

1) The effects of solution selection are algorithm-dependent. For MOEA/D, the selected solutions have larger HV values than the final population on most test problems (25 out of 33). However, NSGA-III with DSS is outperformed by NSGA-III (i.e., the final population) on 15 test problems.
2) The DSS method has negative effects when it is applied to NSGA-III and BiGE on many-objective problems. For example, the final population of NSGA-III is better than the selected solutions by DSS on most 8-objective test problems (9 out of 11) whereas it is better only on a few 3-objective test problems (2 out of 11).
3) The mDTLZ1 test problem is very difficult for NSGA-III and BiGE (compare their average hypervolume values with those by MOEA/D). The use of DSS further deteriorates the performance of those EMO algorithms.

To further investigate why the selected solutions by DSS are worse than the final population, we focus on the single run of NSGA-III on the three-objective mDTLZ1 test problem and the eight-objective DTLZ4 test problem. Fig. 1 shows the solutions in the final population in (a) and the selected solutions in (b) for the three-objective mDTLZ1 test problem. Fig. 2 shows the results on the eight-objective DTLZ4 test problem. The single run with a median hypervolume value of the final population among the 31 runs is chosen in each figure.

In Fig. 1, the top-right plot in each figure shows the solutions closed to the true PF. We can see from Fig. 1 (a) that many solutions in the final population are distributed along the axes (especially the f_1 axis). This is because mDTLZ1 has large hardly dominated regions parallel to each axis. Solutions in those regions are not easy to be dominated by other solutions. In the selected solutions shown in Fig. 1 (b), the situation is even worse. Almost all solutions are distributed along to the three axes. This makes the hypervolume value of the selected solutions significantly smaller than that of the final population.

The negative effect of solution selection by the DSS method can also be clearly observed in Fig. 2. Although the final population converges well to the true PF in $[0, 1]^8$ in Fig. 2 (a), the selected solutions do not converge well in Fig. 2 (b). They are distributed over $[0, 2.4]^8$. That is, there are many selected solutions far from the true PF.

To explain why those poor non-dominated solutions are selected by DSS, we divide the poor non-dominated solutions

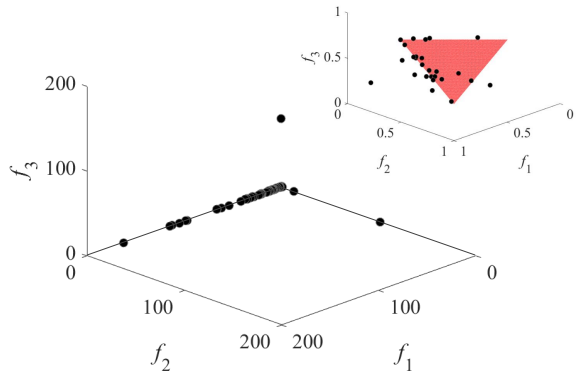

(a) Final population.

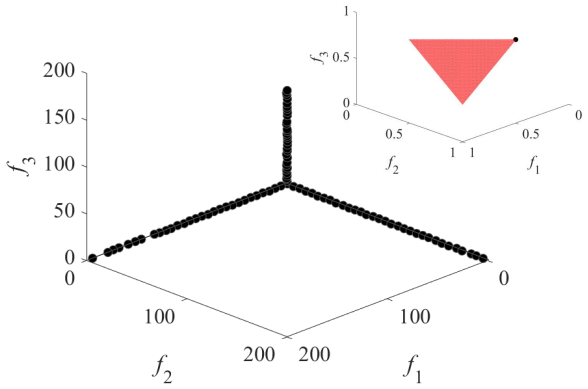

(b) Selected solutions by DSS.

Fig. 1. Solutions in the final population of NSGA-III on the three-objective mDTLZ1 test problem in (a) and the selected solutions by DSS from the UEA in (b). The top-right part of each figure shows the solutions close to the true PF.

shown in Fig. 1 (b) and Fig. 2 (b) into the following two categories: 1) poor non-dominated solutions close to one axis of the objective space, and 2) poor non-dominated solutions not close to any axis. These two types of poor non-dominated solutions are illustrated for a two-objective minimization problem in Fig. 3 (a) and Fig. 3 (b), respectively. The blue points represent the solutions which have already been selected (i.e., in the selected solution subset) and the red points represent the solutions to be selected (i.e., not in the selected solution subset).

In Fig. 3 (a), let us assume that we want to select three solutions from the five red solutions A-E. Since we always select the solution with the largest distance from the selected solution subset, solution E will be selected first. In the next iteration, solution C will be selected. After that, solution D will be selected (since the distance from D to C and E is larger than that between B and the closest blue solution). Whereas solution B is on the true PF and has a larger hypervolume

TABLE II
AVERAGE HV VALUE OF THE FINAL POPULATION AND THE SELECTED SOLUTIONS BY THE DSS METHOD OVER 31 RUNS OF EACH EMO ALGORITHM.

Problem	m	NSGA-III		BiGE		MOEA/D-Tch	
		Final Population	Selected Solutions	Final Population	Selected Solutions	Final Population	Selected Solutions
DTLZ1	3	**8.3864e-01**	8.3589e-1 -	7.7796e-01	**8.3755e-1 +**	8.0184e-01	**8.2327e-1 +**
	5	**9.7836e-01**	9.7631e-1 -	8.7031e-01	**9.7735e-1 +**	9.3739e-01	**9.7839e-1 +**
	8	**9.9684e-01**	9.9565e-1 -	6.9592e-01	**9.9264e-1 +**	9.6096e-01	**9.8621e-1 +**
DTLZ2	3	5.5984e-01	5.5712e-1 =	5.3442e-01	**5.5611e-1 +**	5.2625e-01	**5.4745e-1 +**
	5	**8.1203e-01**	7.9621e-1 -	7.8720e-01	**8.0170e-1 +**	7.1118e-01	**8.1054e-1 +**
	8	**9.1545e-01**	8.8239e-1 -	8.9581e-01	**9.0019e-1 +**	6.2793e-01	**7.9873e-1 +**
DTLZ3	3	3.9724e-01	3.4359e-1 =	**4.7326e-01**	4.2448e-1 -	4.4290e-01	**4.5894e-1 +**
	5	5.8157e-01	5.6458e-1 =	4.4363e-01	**6.5595e-1 +**	7.0412e-01	**7.7341e-1 +**
	8	**6.6229e-01**	4.8058e-1 -	0.0000e+0	0.0000e+0 =	6.2662e-01	6.4956e-1 =
DTLZ4	3	4.9896e-01	4.9818e-1 =	5.0895e-01	**5.1379e-1 +**	3.6075e-01	3.0863e-1 =
	5	**8.0773e-01**	7.8421e-1 -	7.9057e-01	**7.9747e-1 +**	5.7678e-01	**6.8803e-1 +**
	8	**9.0620e-01**	7.5040e-1 -	**9.0715e-01**	7.9592e-1 -	6.3519e-01	**8.0018e-1 +**
IDTLZ1	3	1.9881e-01	**2.1225e-1 +**	2.0040e-01	**2.1744e-1 +**	2.0085e-01	**2.0438e-1 +**
	5	8.0318e-03	**1.0083e-2 +**	1.0909e-02	**1.3013e-2 +**	7.4771e-03	**1.1664e-2 +**
	8	2.6762e-05	2.4765e-5 =	**2.3619e-05**	2.2185e-5 -	1.0000e-05	6.6667e-6 =
IDTLZ2	3	5.2096e-01	**5.3236e-1 +**	5.1836e-01	**5.3286e-1 +**	5.1548e-01	**5.2048e-1 +**
	5	7.6710e-02	**1.0447e-1 +**	**1.2585e-01**	1.2023e-1 -	9.4414e-02	**1.1413e-1 +**
	8	**2.2390e-03**	9.4672e-4 -	**5.1055e-03**	1.7714e-3 -	3.0333e-04	**1.2251e-3 +**
mDTLZ1	3	**6.6930e-02**	6.5890e-3 -	**1.3289e-02**	3.3900e-3 -	**1.9560e-01**	9.0250e-3 -
	5	**5.8440e-04**	1.5569e-6 -	**5.3362e-04**	0.0000e+0 -	**4.1975e-03**	8.0045e-6 -
	8	**4.7076e-08**	0.0000e+0 -	**9.4461e-07**	4.3934e-8 -	0.0000e+00	**1.2355e-8 +**
mDTLZ2	3	5.0942e-01	**5.1821e-1 +**	5.1952e-01	**5.2691e-1 +**	**5.1301e-01**	5.0688e-1 -
	5	4.6861e-02	**5.6964e-2 +**	**1.2573e-01**	9.8087e-2 -	9.0976e-02	**1.0109e-1 +**
	8	**1.6269e-03**	4.5593e-4 -	**5.0922e-03**	1.7115e-3 -	2.3000e-04	**7.3374e-4 +**
DTLZ5IM	3	1.9268e-01	**1.9974e-1 +**	1.9172e-01	**2.0005e-1 +**	1.9503e-01	1.9715e-1 =
	5	6.0026e-01	**6.1172e-1 +**	6.0796e-01	**6.2292e-1 +**	4.7745e-01	**6.2146e-1 +**
	8	**8.0628e-01**	7.6799e-1 -	1.8391e-01	**6.2012e-1 +**	5.8330e-01	**7.0560e-1 +**
DTLZ7	3	2.7257e-01	**2.7524e-1 +**	2.6740e-01	**2.7273e-1 +**	2.2898e-01	**2.4904e-1 +**
	5	2.2340e-01	**2.4442e-1 +**	2.6124e-01	2.6431e-1 =	2.2761e-01	**2.4029e-1 +**
	8	**1.3191e-01**	1.1630e-1 -	2.1166e-01	2.1207e-1 =	2.0768e-01	2.0631e-1 =
WFG2	3	9.2769e-01	9.2818e-1 =	9.2678e-01	**9.3176e-1 +**	8.7088e-01	**9.0668e-1 +**
	5	9.8913e-01	**9.8823e-1 +**	9.9305e-01	**9.9436e-1 +**	9.6720e-01	**9.9360e-1 +**
	8	9.9451e-01	9.9489e-1 =	9.9503e-01	9.9540e-1 =	9.9309e-01	**9.9698e-1 +**
+/-/=			11/15/7		19/10/4		25/3/5

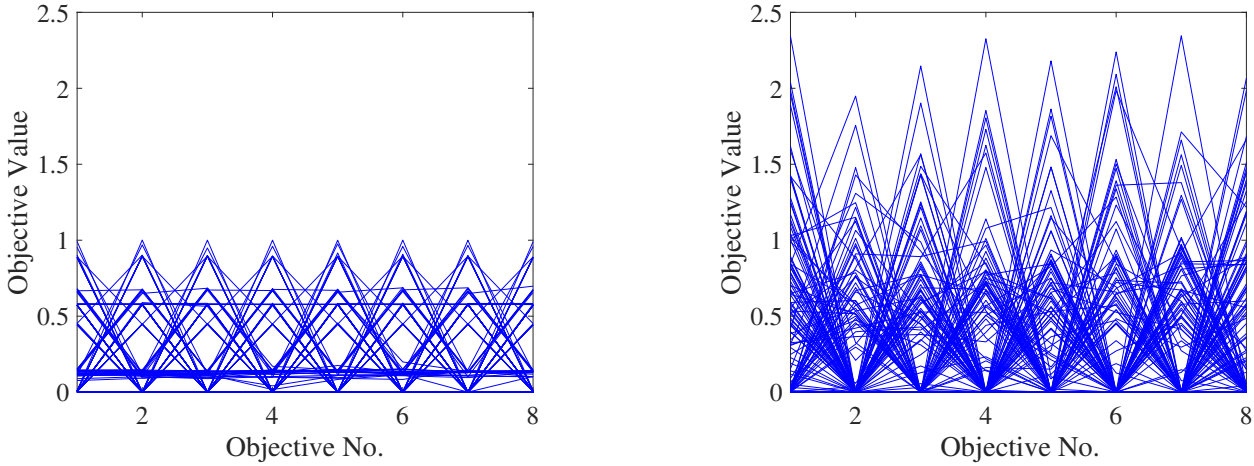

(a) final population.

(b) Selected solutions by DSS.

Fig. 2. Solutions in the final population of NSGA-III on the eight-objective DTLZ4 test problem in (a) and the selected solutions by DSS from the UEA in (b).

contribution than solution D, it is not selected. This explains why many solutions along the three axes are selected but many solutions close to the true PF are not selected by DSS in Fig. 1 (b).

In Fig. 3 (b), let us assume that we have already selected the four blue solutions and we want to select one more solution from F and G. The DSS method chooses G since G has the larger distance from the selected blue solutions than F. This explains why some poor non-dominated solutions are selected whereas they are not close to any axis. This type of poor non-dominated solutions are not common in two- and three-objective problems since they are easily dominated by other solutions. However, it is likely that those solutions exist in the UEA of a many-objective problem. This is because solutions are very sparse in the objective space even when all non-dominated solutions are stored in the UEA.

DSS from the true PF was proven to be conditionally equivalent for hypervolume maximization [14]. However, in real-world applications, non-dominated solutions in the UEA are not always on the true PF, especially when the problem is many-objective or difficult to solve. Non-dominated solutions in the UEA can be far from the true PF. Whereas they are not good solutions, they often have large distances from the selected solutions. As a result, they are likely to be selected whereas they are not good solutions since they are far away from the true PF.

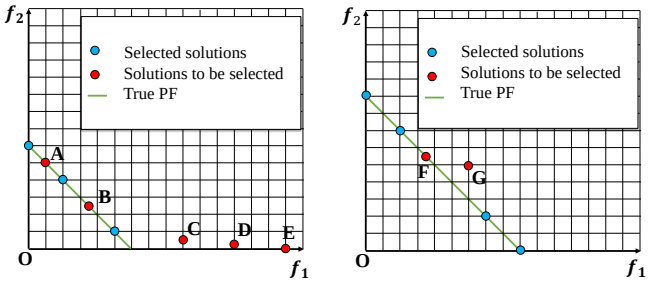

(a) Close to one axis. (b) Not close to any axis.

Fig. 3. Two types of poor non-dominated solutions.

III. Modified Distance-based Subset Selection

A. Modification

In the DSS method, the Euclidean distance $d(a, z)$ is used, which is calculated by the following formula:

$$d(a,z) = (\sum_{i=1}^{m} (z_i - a_i)^2)^{1/2}. \quad (1)$$

However, subset selection based on the Euclidean distance has some difficulties as shown in the last section. To remedy those difficulties of the DSS method, we propose a new subset selection method based on IGD$^+$ distance [22], which is defined by the distance from a to the region dominated by z. The formula to calculate the IGD$^+$ distance between two points is as follows:

$$d^+(a,z) = (\sum_{i=1}^{m} (max\{z_i - a_i, 0\})^2)^{1/2}. \quad (2)$$

Fig. 4 illustrates the difference between d in (1) and d^+ in (2). In Fig. 4, a dominates z for a two-objective minimization problem, which means that z_i is larger than or equal to a_i (i.e., $z_i - a_i$ is always non-negative). Thus, $d^+(a, z)$ is the same as $d(a, z)$. For another solution b, b and z are non-dominated. Since $z_1 - b_1$ is smaller than 0, we only calculate the positive part $z_2 - b_2$. In this case, $d^+(b, z)$ is different from $d(b, z)$. Only the positive elements of $d(b, z)$ remain in $d^+(b, z)$.

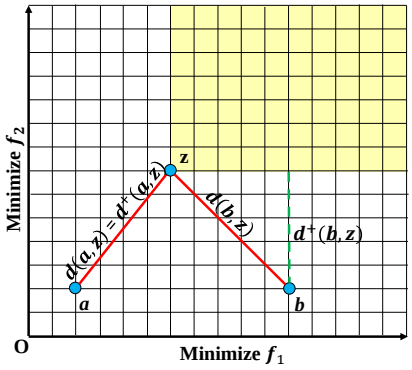

Fig. 4. Illustration of the difference between the Euclidean distance and the IGD$^+$ distance. The yellow region is the region dominated by z.

By using the IGD$^+$ distance instead of the Euclidean distance, we can obtain different solution subset selection results. Fig. 5 shows the IGD$^+$ distance from each solution to be selected to the selected solution set. In Fig. 5 (a), we can see that although C, D, E have large Euclidean distance to the selected solution set, their IGD$^+$ distances are not large. Instead, solution B has the largest IGD$^+$distance to the selected solution set. Thus, solution B is selected first and then solution A and E are selected. Comparing with the solution selected by the Euclidean distance, IGD$^+$ distance-based selection can avoid selecting too many points close to the axis and far from the true PF.

In Fig. 5 (b), solution G is selected if we use the Euclidean Distance. However, if we use the IGD$^+$ distance, solution F is selected since F has a larger IGD$^+$ distance than G from the selected blue solutions. It is obvious that F is closer to the true PF and is a better solution than G. As explained in Fig. 5 (b), the use of the IGD$^+$ distance can also avoid selecting poor non-dominated solutions which are not close to any axis.

From the above examples, we can see that the use of the IGD$^+$ distance for solution selection works as a countermeasure against the negative effects of the DSS method. Except for the use of the IGD$^+$ distance, the proposed solution selection method is exactly the same as the DSS method in [14]. The details of the proposed IGD$^+$ distance-based solution subset selection method are shown in Algorithm 2.

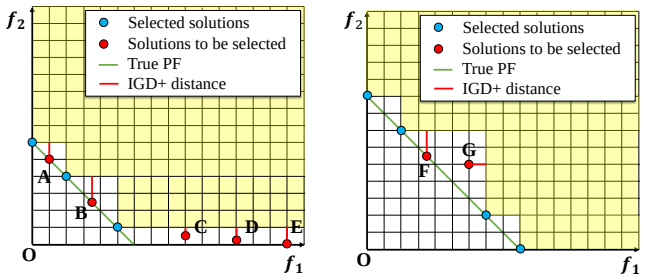

(a) Close to one axis. (b) Not close to any axis.

Fig. 5. Minimal IGD^+ distance of each non-dominated solution to be selected.

Algorithm 2 IGD^+ Distance-Based Subset Selection (DSS^+)

Input: A (A set of non-dominated solutions in UEA),
k (Solution subset size)
Output: P (A set of selected solutions)
if $|A| < k$ **then**
  $P = A$
else
  Normalize all solutions in A to $[0, 1]$
  Sort A based on the crowding distance
  Initialize P as the first solution in the sorted archive A
  while $|A| < k$ **do**
    for each a_i in $A \setminus P$ **do**
      D_i= minimum IGD^+distance from a_i to any point in P
    end for
    Choose a solution from $A \setminus P$ associated with the largest IGD^+distance and add it to P
  end while
end if

B. Experimental Results

In the same manner as the computational experiments in the previous section, we perform solution selection using the IGD^+ distance-based solution subset selection method. That is, the following two methods are compared:

1) Euclidean distance-based subset selection (DSS) from all non-dominated solutions stored in UEA.
2) IGD^+ distance-based subset selection (DSS^+) from all non-dominated solutions stored in UEA.

Table III shows the performance comparison results of these two methods. The bolded value indicates that one selection method is significantly better than the other by the Wilcoxon rank sum test.

As shown in Table III, the DSS^+ method is significantly better than the DSS method on about half cases (48 out of 99 cases: three algorithms, 11 problems and three settings of the number of objectives). There is no significant difference between DSS^+ and DSS on most of the remaining cases (49 cases). DSS^+ is outperformed by DSS only on two cases for solution selection from the UEA of MOEA/D.

From Table III, we can observe that there is no significant difference between DSS and DSS^+ method on all three-objective problems with the regular PF (i.e., DTLZ1-4). However, when the number of objects increases from three to five and eight, DSS^+ outperforms DSS on some of those test problems (5 out of 8 for NSGA-III, 3 out of 8 for BiGE, and 2 out of 8 for MOEA/D).

Fig. 6 shows the selected solutions by DSS^+ from the UEA of NSGA-III on the eight-objective DTLZ4 problem. We use the same single run of NSGA-III as in Fig. 2. That is, we use the same UEA in Fig. 2 and Fig. 6. We can observe some solutions which are not close to the true PF (which is in $[0, 1]^8$) in Fig. 6. However, the number of those solutions clearly decreases from Fig. 2 (b). As a result, the average HV value of the selected solutions by DSS^+ from the UEA of NSGA-III on the eight-objective DTLZ4 is significantly improved from that by DSS in Table III.

For the test problems with the inverted PF, especially for mDTLZ1, DSS^+ is significantly better than DSS in Table III. The average HV value by DSS^+ is hundreds of times larger than that by DSS for mDTLZ1. Fig. 7 shows the selected solutions by DSS^+ from the UEA of NSGA-III on the three-objective mDTLZ1 problem. The same UEA is used in Fig. 1 (b) and Fig. 7. Compared with the selected solutions in Fig. 1 (b), we can see that the number of poor non-dominated solutions close to each axis is clearly decreased by DSS^+. Much more solutions close to the true PF are selected in Fig. 7 by DSS^+ than in Fig. 1 (b) by DSS. It is interesting to observe that more solutions close to the true PF are obtained by solution selection from the UEA by DSS^+ in Fig. 7 than the final population in Fig. 1 (a).

While DSS^+ performs better than DSS even on some many-objective test problems with the regular PF, DSS and DSS^+ have no significant difference on some other many-objective test problems. For example, the average HV values by NSGA-III with DSS and NSGA-III with DSS^+ have no significant difference on the 8-objective DTLZ1 problem. As we have already explained, DSS^+ can avoid choosing too many points far away from PF. However, if no selected solution by DSS is far away from the true PF, DSS and DSS^+ have no large difference in their performance.

In Table III, we can also see that MOEA/D with DSS^+ performs worse than DSS on two problems: DTLZ1 and DTLZ3. To further investigate the reason for the performance deterioration, we show the selected solution sets by MOEA/D with DSS and DSS^+ on the eight-objective DTLZ1 problem of a single run in Fig. 8. We can see that no poor non-dominated solutions are selected by DSS in Fig. 8. Thus, DSS^+ is not needed. The reason for the slightly worse performance of DSS^+ than DSS for MOEA/D on the eight-objective DTLZ1 may be the slightly worse uniformity of the selected solutions by DSS^+ than DSS (see Fig. 8).

IV. Conclusion

In this paper, we first compared the final population with the selected solutions by the DSS method and showed that DSS has some difficulties in the handling of non-dominated

TABLE III
AVERAGE HV VALUE OF THE SELECTED SOLUTIONS BY THE DSS AND DSS$^+$ METHODS OVER 31 RUNS OF EACH EMO ALGORITHM.

Problem	m	NSGA-III		BiGE		MOEA/D-Tch	
		DSS	DSS+	DSS	DSS+	DSS	DSS+
DTLZ1	3	8.3589e-1	8.3653e-1 =	8.3755e-1	8.3884e-1 =	8.2327e-1	8.2600e-1 =
	5	9.7631e-1	**9.7850e-1 +**	9.7735e-1	9.7784e-1 =	9.7839e-1	**9.7930e-1 +**
	8	9.9565e-1	9.9424e-1 =	9.9264e-1	9.9460e-1 =	**9.8621e-1**	9.7523e-1 -
DTLZ2	3	5.5712e-1	5.5551e-1 =	5.5611e-1	5.5754e-1 =	5.4745e-1	5.5021e-1 =
	5	7.9621e-1	**8.0196e-1 +**	8.0170e-1	**8.0609e-1 +**	8.1054e-1	8.1205e-1 =
	8	8.8239e-1	**9.0595e-1 +**	9.0019e-1	**9.0968e-1 +**	7.9873e-1	**8.3771e-1 +**
DTLZ3	3	3.4359e-1	3.2774e-1 =	4.2448e-1	4.3129e-1 =	4.5894e-1	4.5527e-1 =
	5	5.6458e-1	5.0551e-1 =	6.5595e-1	7.0519e-1 =	**7.7341e-1**	7.4749e-1 -
	8	4.8058e-1	4.9659e-1 =	0.0000e+0	0.0000e+0 =	6.4956e-1	6.3369e-1 =
DTLZ4	3	4.9818e-1	4.5383e-1=	5.1379e-1	5.4118e-1 =	3.0863e-1	**4.2145e-1 +**
	5	7.8421e-1	**7.9653e-1 +**	7.9747e-1	8.0620e-1 =	6.8803e-1	6.6255e-1 =
	8	7.5040e-1	**9.0662e-1 +**	7.9592e-1	**9.1715e-1 +**	8.0018e-1	8.1531e-1 =
IDTLZ1	3	2.1225e-1	2.1358e-1 =	2.1744e-1	2.1678e-1 =	2.0438e-1	2.0742e-1 =
	5	1.0083e-2	1.0365e-2 =	1.3013e-2	1.2358e-2 =	1.1664e-2	1.1836e-2 =
	8	2.4765e-5	2.8434e-5 =	2.2185e-5	3.2330e-5 =	6.6667e-6	6.6666e-6 =
IDTLZ2	3	5.3236e-1	5.3048e-1 =	5.3286e-1	5.3397e-1 =	5.2048e-1	**5.2520e-1 +**
	5	1.0447e-1	**1.1986e-1 +**	1.2023e-1	**1.3183e-1 +**	1.1413e-1	**1.2507e-1 +**
	8	9.4672e-4	**2.5993e-3 +**	1.7714e-3	**4.5643e-3 +**	1.2251e-3	**2.1840e-3 +**
mDTLZ1	3	6.5890e-3	**1.7817e-1 +**	3.3900e-3	**1.3760e-1 +**	9.0250e-3	**2.0385e-1 +**
	5	1.5569e-6	**4.2130e-3 +**	0.0000e+0	**3.2533e-3 +**	8.0045e-6	**7.4473e-3 +**
	8	0.0000e+0	**2.0558e-8 +**	4.3934e-8	**9.4245e-7 +**	1.2355e-8	**5.7036e-7 +**
mDTLZ2	3	5.1821e-1	**5.2708e-1 +**	5.2691e-1	**5.3202e-1 +**	5.0688e-1	**5.2059e-1 +**
	5	5.6964e-2	**1.0225e-1 +**	9.8087e-2	**1.3065e-1 +**	1.0109e-1	**1.2112e-1 +**
	8	4.5593e-4	**2.0865e-3 +**	1.7115e-3	**4.5190e-3 +**	7.3374e-4	**1.9601e-3 +**
DTLZ5IM	3	1.9974e-1	1.9878e-1 =	2.0005e-1	1.9798e-1 =	1.9715e-1	1.9646e-1 =
	5	6.1172e-1	**6.1899e-1 +**	6.2292e-1	**6.2503e-1 +**	6.2146e-1	6.1713e-1 =
	8	7.6799e-1	7.5273e-1 =	6.2012e-1	6.0164e-1 =	7.0560e-1	7.1717e-1 =
DTLZ7	3	2.7524e-1	**2.7631e-1 +**	2.7273e-1	2.7502e-1 =	2.4904e-1	2.4698e-1 =
	5	2.4442e-1	**2.5988e-1 +**	2.6431e-1	**2.7947e-1 +**	2.4029e-1	2.3657e-1 =
	8	1.1630e-1	**1.4441e-1 +**	2.1207e-1	**2.2977e-1 +**	2.0631e-1	2.0489e-1 =
WFG2	3	9.2818e-1	**9.3204e-1 +**	9.3176e-1	**9.3525e-1 +**	9.0668e-1	9.0817e-1 =
	5	9.8823e-1	9.8923e-1 =	9.9436e-1	**9.9512e-1 +**	9.9360e-1	**9.9491e-1 +**
	8	9.9489e-1	9.9579e-1 =	9.9540e-1	**9.9625e-1 +**	9.9698e-1	9.9734e-1 =
+/-/=			18/0/15		17/0/16		13/2/18

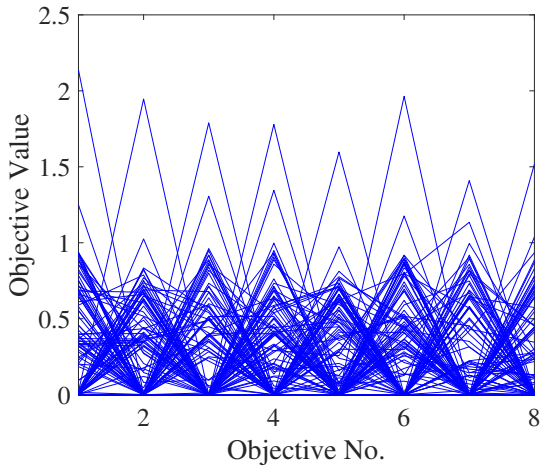

Fig. 6. Selected solutions by DSS$^+$ from the UEA of NSGA-III on the eight-objective DTLZ4 problem.

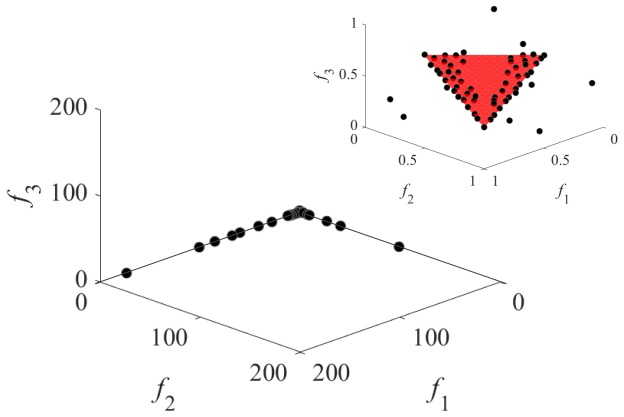

Fig. 7. Selected solutions by DSS$^+$ from the UEA of NSGA-III on the three-objective mDTLZ1 problem.

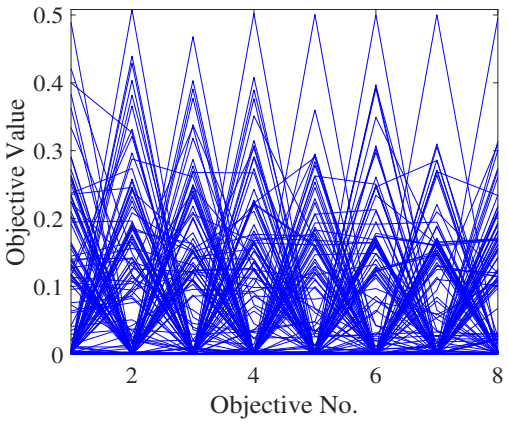

(a) Selected Solutions by DSS Method.

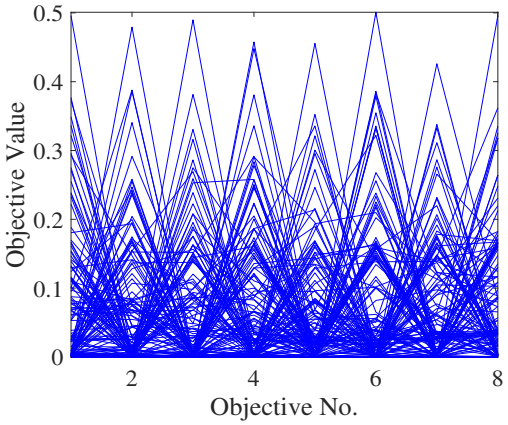

(b) Selected Solutions by DSS$^+$ Method.

Fig. 8. Selected solutions by DSS in (a) and DSS$^+$ in (b) from the UEA of MOEA/D-Tch on the eight-objective DTLZ1 problem.

solutions far away from the true Pareto front. Then, a new subset selection method based on IGD$^+$ distances was proposed. In the proposed method, IGD$^+$ distance was used to avoid selecting too many poor non-dominated solutions far away from the true PF. Our experimental results demonstrated that DSS$^+$ is significantly better than DSS or at least equal to DSS on most of the examined benchmark problems, especially on many-objective problems or test problems with inverted PFs.

Since the usefulness of DSS$^+$ and DSS seems to depend on the problem and the EMO algorithm, it will be an interesting future research topic to further examine the relationship between the usefulness of solution selection (by DSS and DSS$^+$) and characteristic feature of the EMO algorithm and the test problem. Of course, the proposal of new solution selection methods (including further modifications of the DSS method) is an interesting future research topic.

REFERENCES

[1] K. Deb, A. Pratap, S. Agarwal, and T. Meyarivan, "A fast and elitist multiobjective genetic algorithm: Nsga-II," *IEEE Transactions on Evolutionary Computation*, vol. 6, no. 2, pp. 182–197, April 2002.

[2] K. Deb and H. Jain, "An evolutionary many-objective optimization algorithm using reference-point-based nondominated sorting approach, part I: Solving problems with box constraints," *IEEE Transactions on Evolutionary Computation*, vol. 18, no. 4, pp. 577–601, Aug 2014.

[3] Q. Zhang and H. Li, "MOEA/D: A multiobjective evolutionary algorithm based on decomposition," *IEEE Transactions on Evolutionary Computation*, vol. 11, no. 6, pp. 712–731, Dec 2007.

[4] R. Cheng, Y. Jin, M. Olhofer, and B. Sendhoff, "A reference vector guided evolutionary algorithm for many-objective optimization," *IEEE Transactions on Evolutionary Computation*, vol. 20, no. 5, pp. 773–791, Oct 2016.

[5] E. Zitzler and S. Künzli, "Indicator-based selection in multiobjective search," in *International conference on parallel problem solving from nature*. Springer, 2004, pp. 832–842.

[6] J. Bader and E. Zitzler, "HypE: An algorithm for fast hypervolume-based many-objective optimization," *Evolutionary Computation*, vol. 19, no. 1, pp. 45–76, March 2011.

[7] R. Tanabe, H. Ishibuchi, and A. Oyama, "Benchmarking multi- and many-objective evolutionary algorithms under two optimization scenarios," *IEEE Access*, vol. 5, pp. 19 597–19 619, 2017.

[8] H. Ishibuchi, Y. Setoguchi, H. Masuda, and Y. Nojima, "How to compare many-objective algorithms under different settings of population and archive sizes," in *2016 IEEE Congress on Evolutionary Computation (CEC)*, July 2016, pp. 1149–1156.

[9] K. Bringmann, T. Friedrich, and P. Klitzke, "Generic postprocessing via subset selection for hypervolume and epsilon-indicator," in *International Conference on Parallel Problem Solving from Nature*. Springer, 2014, pp. 518–527.

[10] T. Kuhn, C. M. Fonseca, L. Paquete, S. Ruzika, M. M. Duarte, and J. R. Figueira, "Hypervolume subset selection in two dimensions: Formulations and algorithms," *Evolutionary Computation*, vol. 24, no. 3, pp. 411–425, Sep. 2016.

[11] A. P. Guerreiro, C. M. Fonseca, and L. Paquete, "Greedy hypervolume subset selection in the three-objective case," in *Proceedings of the 2015 Annual Conference on Genetic and Evolutionary Computation*, 2015, pp. 671–678.

[12] K. Bringmann and T. Friedrich, "Approximating the volume of unions and intersections of high-dimensional geometric objects," *Computational Geometry*, vol. 43, no. 6-7, pp. 601–610, 2010.

[13] Q. Zhang, W. Liu, and H. Li, "The performance of a new version of MOEA/D on CEC09 unconstrained MOP test instances," in *2009 IEEE Congress on Evolutionary Computation*, May 2009, pp. 203–208.

[14] H. K. Singh, K. S. Bhattacharjee, and T. Ray, "Distance-based subset selection for benchmarking in evolutionary multi/many-objective optimization," *IEEE Transactions on Evolutionary Computation*, vol. 23, no. 5, pp. 904–912, Oct 2019.

[15] K. Deb, L. Thiele, M. Laumanns, and E. Zitzler, "Scalable multi-objective optimization test problems," in *Proceedings of the 2002 Congress on Evolutionary Computation. CEC'02 (Cat. No.02TH8600)*, vol. 1, May 2002, pp. 825–830 vol.1.

[16] H. Jain and K. Deb, "An evolutionary many-objective optimization algorithm using reference-point based nondominated sorting approach, part II: Handling constraints and extending to an adaptive approach," *IEEE Transactions on Evolutionary Computation*, vol. 18, no. 4, pp. 602–622, Aug 2014.

[17] Z. Wang, Y. Ong, and H. Ishibuchi, "On scalable multiobjective test problems with hardly dominated boundaries," *IEEE Transactions on Evolutionary Computation*, vol. 23, no. 2, pp. 217–231, April 2019.

[18] S. Huband, P. Hingston, L. Barone, and L. While, "A review of multiobjective test problems and a scalable test problem toolkit," *IEEE Transactions on Evolutionary Computation*, vol. 10, no. 5, pp. 477–506, Oct 2006.

[19] K. Deb and D. K. Saxena, "On finding pareto-optimal solutions through dimensionality reduction for certain large-dimensional multi-objective optimization problems," *Kangal report*, vol. 2005011, 2005.

[20] K. Deb and S. Tiwari, "Omni-optimizer: A generic evolutionary algorithm for single and multi-objective optimization," *European Journal of Operational Research*, vol. 185, no. 3, pp. 1062–1087, 2008.

[21] E. Zitzler and L. Thiele, "Multiobjective optimization using evolutionary algorithms¡ªa comparative case study," in *International Conference on Parallel Problem Solving from Nature*. Springer, 1998, pp. 292–301.

[22] H. Ishibuchi, H. Masuda, Y. Tanigaki, and Y. Nojima, "Modified distance calculation in generational distance and inverted generational distance," in *International Conference on Evolutionary Multi-criterion Optimization*. Springer, 2015, pp. 110–125.